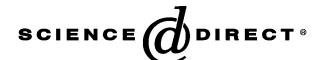


Available online at www.sciencedirect.com





Palaeogeography, Palaeoclimatology, Palaeoecology 231 (2006) 169-180

www.elsevier.com/locate/palaeo

Glacial morphology and sediment formation in the Mertz Trough, East Antarctica

Katherine McMullen ^{a,*}, Eugene Domack ^a, Amy Leventer ^b, Caroline Olson ^b, Robert Dunbar ^c, Stefanie Brachfeld ^d

a Department of Geosciences, Hamilton College, Clinton, NY 13323, USA
 b Department of Geology, Colgate University, Hamilton, NY 13346, USA
 c Department of Geological and Environmental Sciences, Stanford University, Stanford, CA 94305, USA
 d Department of Geology, Montclair State University, Upper Montclair, NJ 07043, USA

Accepted 8 July 2005

Abstract

The *Nathaniel B. Palmer* 01-01 cruise produced a SeaBeam map showing unprecedented detail of the bathymetry in the Mertz Trough of East Antarctica. In addition, seismic reflection surveys and sediment core collection were completed in the region. The morphology of the Mertz Trough is combined with core data to interpret the sequence of events that occurred in this area since the Last Glacial Maximum. These complementary data indicate that an ice sheet once covered the Mertz Trough, which deposited diamicton and formed mega-scale glacial lineations during glacial maximal conditions and grounding-line wedges during recession. An erosional feature caused by subglacial meltwater breaching at least one of the grounding-line deposits is also recognized, along with a fan of sediment deposited seaward of the breach. Sediment cores from the Mertz Trough consist of two distinct units, the diamicton deposited subglacially and a diatom mud and ooze, deposited after the ice retreated. The latter unit has been preferentially deposited in deeper areas of the trough as a hemipelagic drape and shows that a change in the nature of the diatom unit occurred about 3300 ¹⁴C yr BP.

 $\ensuremath{\mathbb{C}}$ 2005 Elsevier B.V. All rights reserved.

Keywords: Antarctica; Bathymetry; Deglaciation; Glacial geology; Glaciomarine sedimentation; Ice streams

1. Introduction

Underwater troughs and banks dominate the Wilkes Land continental shelf of East Antarctica. Troughs occur seaward of major glacial outlets where ice-flow converges and where velocity increases, ice streams can form (Anderson et al., 2001; Wellner et al., 2001). Evidence of past ice streaming is shown by the presence of mega-scale glacial lineations. In West Antarctica, it

E-mail address: kmcmulle@hamilton.edu (K. McMullen).

have ice sheet profiles that are generally low and the ice sheet usually terminates in an ice shelf (Anderson et al., 2001), which is believed to have happened in the Mertz Trough. As ice sheets become unstable, they change in size. Instability can occur because of a rise in sea level and/or thinning of the margin, both of which result in landward retreat of the ice margin (Anderson et al., 2001). This retreat could occur gradually (Domack et al., 1999) and/or episodically, or catastrophically. As ice retreated in the Mertz Trough, it paused in at least two locations leaving grounding-line wedge deposits. Grounding-line wedges consist of dipping beds of dia-

has been shown that areas with maximum discharge

^{*} Corresponding author. Tel.: +1 315 859 4699; fax: +1 315 859 4744.

micton overlain by horizontal layers of diamicton (Benn and Evans, 1998). They are formed from sediment that is transported beneath the glacier towards its margin and are deposited when ice pauses during its retreat (Anderson et al., 2001). Grounding-line wedges form as ice pushes subglacial debris at the grounding line, deforming sedimentary beds and originating gravity flows, which add layers of sediment to the ice-distal side of the wedge (Powell and Domack, 2002). Another source

of sediment in grounding-line wedges is from undermelt of an ice shelf (Powell and Domack, 2002). Both megascale glacial lineations and grounding-line wedges are present in the Mertz Trough and are composed of diamicton with overlying diatomaceous sediments.

The Mertz Trough is located off the George V Coast of Wilkes Land to the northeast of the Mertz Glacier Tongue and to the north of the Ninnis Glacier Tongue, covering an area of about 5000 km² (Fig. 1). It was

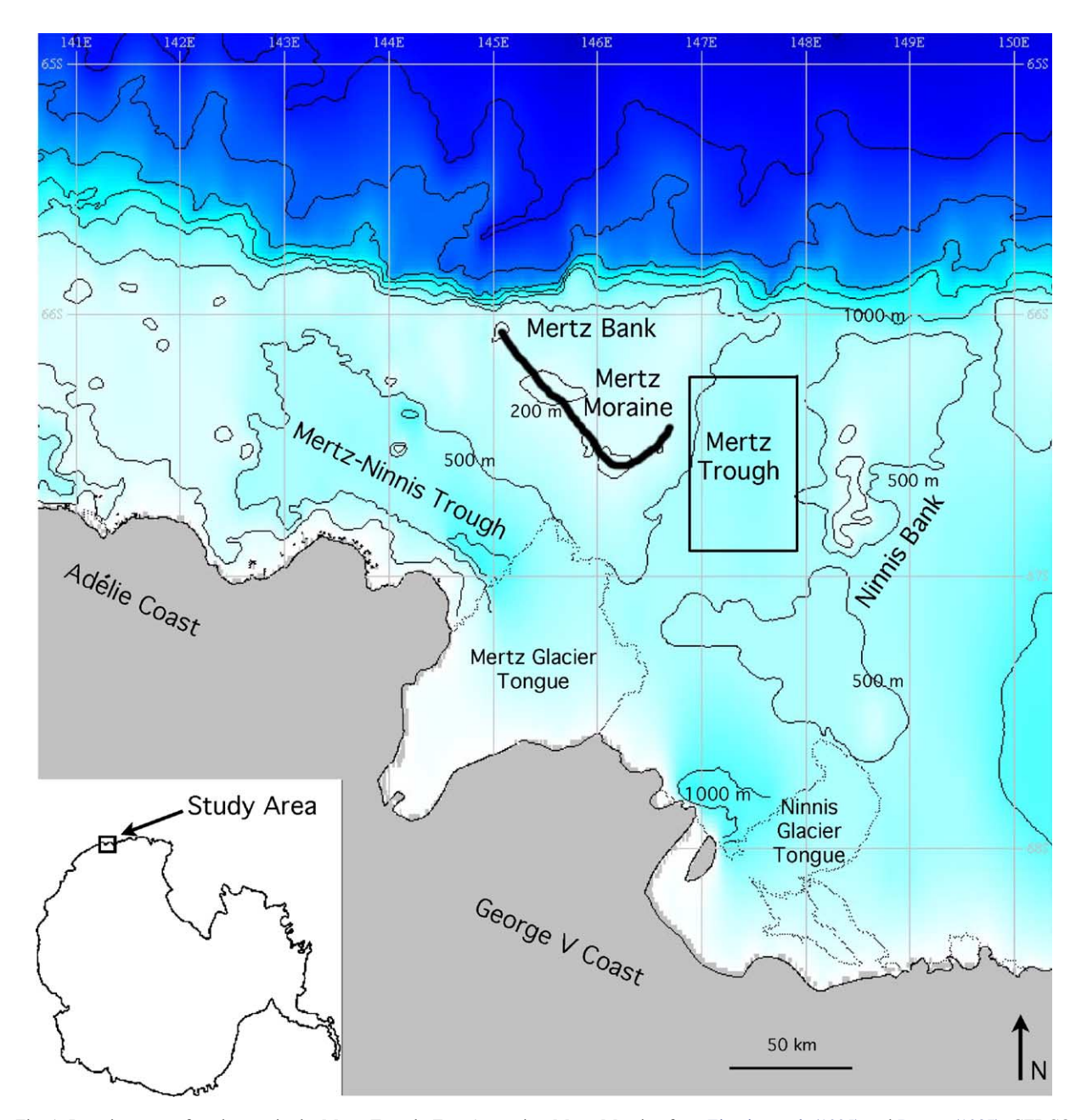


Fig. 1. Location map of study area in the Mertz Trough, East Antarctica. Mertz Moraine from Eittreim et al. (1995) and Barnes (1987). GEBCO bathymetric contours in 500 m intervals, also included is 200 m contour line.

initially mapped and cored during Deep Freeze 1979 (Domack, 1987). Glacial and glacial-marine sediments were found to dominate the subsurface and the regional ice-flow direction was interpreted to be to the northwest (Domack, 1987). Additional knowledge of the bathymetry of the Mertz Trough was acquired during an U.S. Geological Survey cruise in 1984 (Barnes, 1987). With this study, it was concluded that the sea floor morphology of the Mertz Bank and Mertz Trough consists of shoals, grooves, ice gouges, and depressions shaped by glacial ice and icebergs. The ridge and groove topography of the Mertz Trough was interpreted as a subglacially fluted surface and thus was used to reconstruct the ice-flow direction as being parallel to the ridges and grooves in a north-northeast direction, modifying Domack's (1987) interpretation. A joint Australian/Italian survey off the George V Coast was taken during February and March 2000, which attained high-resolution digital bathymetry (Porter-Smith, 2003). During January and February of 2001 the Nathaniel B. Palmer (NBP) 00-08 and 01-01 cruises, studied the Mertz Trough. Bathymetric mapping of the trough was completed, in addition to a seismic reflection survey, complemented by four kasten cores. Scientists aboard both of these cruises produced a swath map showing unprecedented detail of the bathymetry of the trough.

The objective of this paper is to interpret the glacial history of the Mertz Trough using new data obtained on the NBP01-01 cruise. A more detailed map showing trough bathymetry illustrates features that have never been mapped here before and that are instrumental in determining the area's history of past glacial events. Using stratigraphic principles of cross-cutting relationships, it has been possible to propose a detailed sequence of events for the deglaciation of the region.

2. Methods

2.1. SeaBeam data

Sea floor bathymetry data was obtained with a hull-mounted SeaBeam 2112 multibeam sonar system. During bathymetric surveys, ship speed was between 5 and 8 knots. Bathymetry data were corrected for velocity variations. Data were processed on board and printed as contoured and shaded relief maps with a scale of 1:65,600.

2.2. Seismic data

High-resolution seismic reflection profiles were obtained with a hull-mounted ODEC Bathy2000 dual

channel chirp sonar system. The nominal vertical resolution of the Bathy2000 is 8 cm using the highest frequency range of 12–200 kHz. A depth scale of the seismic profiles was calculated by converting two-way travel time using the velocity of sound through water. This scale was continued through the sediment to obtain relative depths.

2.3. Sedimentologic data

Four kasten cores (3 m core barrel) were taken in the Mertz Trough during the NBP01-01 cruise (Table 1). The kasten cores were described, photographed, sampled, and analyzed for magnetic susceptibility onboard. Description of sedimentary structures, fossil content, sediment type and color were made soon after the cores were opened. Photographs were taken before subsampling. Samples were obtained for ¹⁴C dating and for sedimentological, geochemical, and paleontological analyses. Archive trays of the cores were taken and transported to Florida State University Antarctic Research Facility to be X-rayed and stored.

Mass normalized magnetic susceptibility of freezedried sediment was measured on an AGICO KLY-2 Kappabridge sensor at Colgate University. Samples were measured three times and an average was used to calculate the magnetic susceptibility. The mass normalized magnetic susceptibility data of cores KC-1, KC-2, KC-12, and KC-13 are used to help determine sedimentary units in the Mertz Trough.

Ice-rafted debris counts were made on KC-1, KC-2, KC-12, and KC-13 using X-radiographs of the archive trays. Grains larger than 2 mm were counted in 2.5 cm intervals throughout each core following the method of Grobe (1987).

Grain size was analyzed on the top 100 cm of cores KC-1, KC-12, and KC-13 to determine size changes in the mud fraction of the upper unit. Samples were prepared in an ultrasonic cleaner with Calgon to separate individual grains and allow for accurate size analysis using a Malvern Mastersizer E.

Table 1 Location of kasten cores in the Mertz Trough

Core	Latitude	Longitude	Length (cm)	Water depth (m)
KC-1	66 32.312'S	147 25.149'E	261	639
KC-2	66 33.127'S	147 00.249'E	252	544
KC-12	66 39.307'S	147 17.168'E	228	610
KC-13	66 42.757'S	147 08.525′E	251	645

Quantitative diatom slides were prepared at 10 cm intervals for KC-12 and KC-13 using a random settling technique described by Scherer (1995) and Norland 61 optical adhesive. Diatom valves were counted at 1000× magnification using an Olympus BX60 microscope. Diatom valves were counted along transects until a minimum of 400 valves were counted.

3. Results

The Mertz Trough shows evidence of glacial deposition in the form of streamlined elongated ridges, known as mega-scale glacial lineations (after Shipp et al., 1999) including bundles (Canals et al., 2000), and grounding-line wedges (after Powell and Domack, 2002). These glacial seafloor features in turn are

NBP0101 SeaBeam Edited Data - Mertz Trough

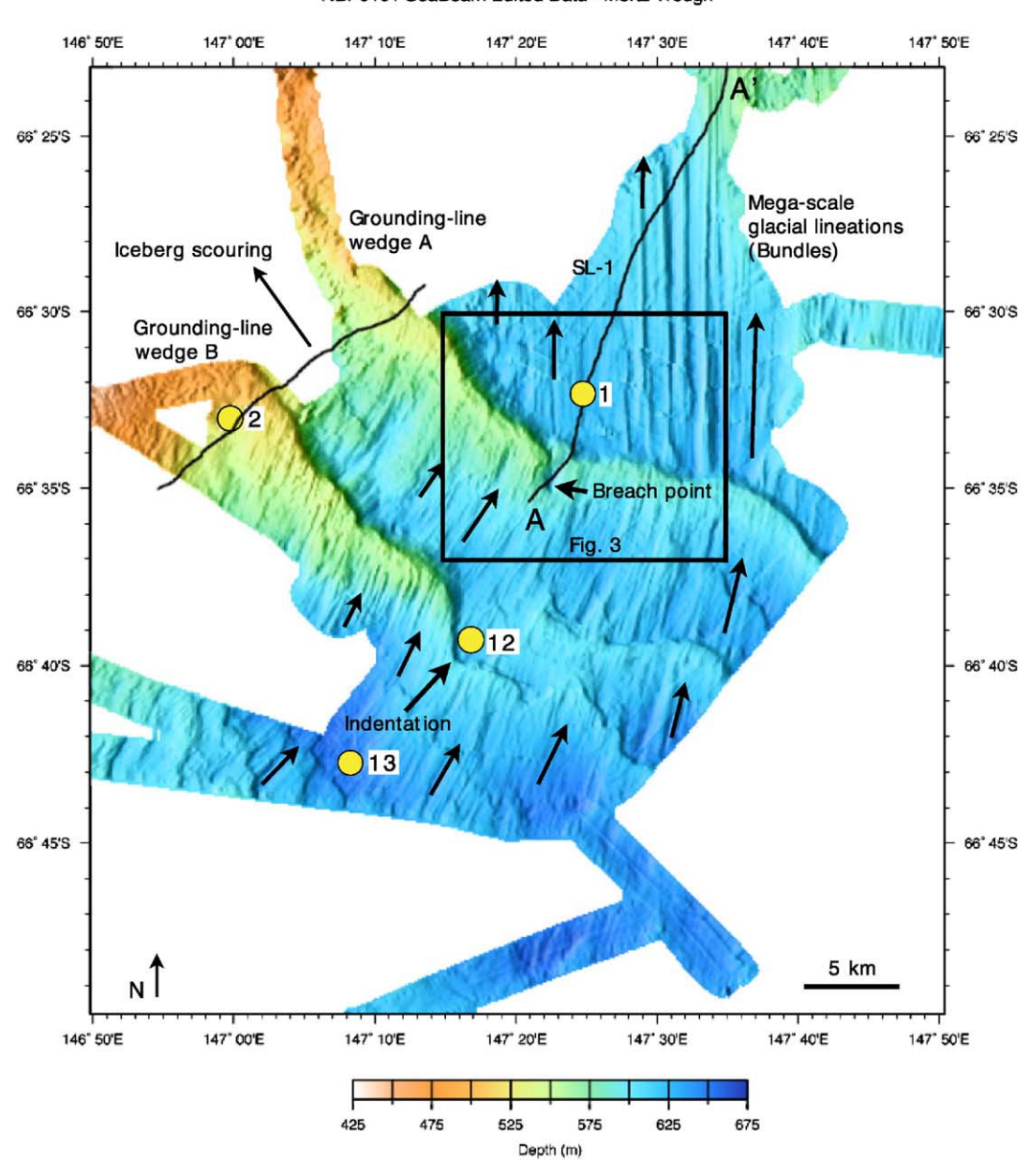


Fig. 2. Bathymetry map of the Mertz Trough. Areas of mega-scale glacial lineations and grounding-line wedges are shown. Arrows represent interpreted flow directions. Location of seismic line and kasten cores (KC-1, KC-2, KC-12, and KC-13) are also shown. Iceberg scouring is seen to the northwest of the line shown.

used to divide the region into two morphological areas (Fig. 2).

3.1. Morphology

3.1.1. Mega-scale glacial lineations

The seafloor of the northern part of the survey is characterized by 4–5 parallel streamlined ridges, 14–20 km long, about 500 m wide, and 20 m high (Fig. 2). They are oriented in a north-south direction and are spaced at a distance of 1–1.5 km crest-to-crest. These features are similar to, although smaller than, the bundle structures observed in the Gerlache Strait by Canals et al. (2000). In the Ross Sea, streamlined, elongated

ridges such as these have been referred to simply as mega-scale glacial lineations, which typically range from 8–70 km in length and 200–1300 m in width, with crest-to-crest distances between ridges of 0.3–5 km (Shipp et al., 1999). According to Anderson et al. (2001), these ridges are confined to glacial troughs and lie parallel to the trough axis.

3.1.2. Grounding-line wedges

The Mertz Trough presents two distinct groundingline wedges, designated A and B in Fig. 2, which have a general northwest-southeast orientation. They lie over 30 km in length and up to 80 m in height. The northeastern sides of the grounding-line wedges are steep

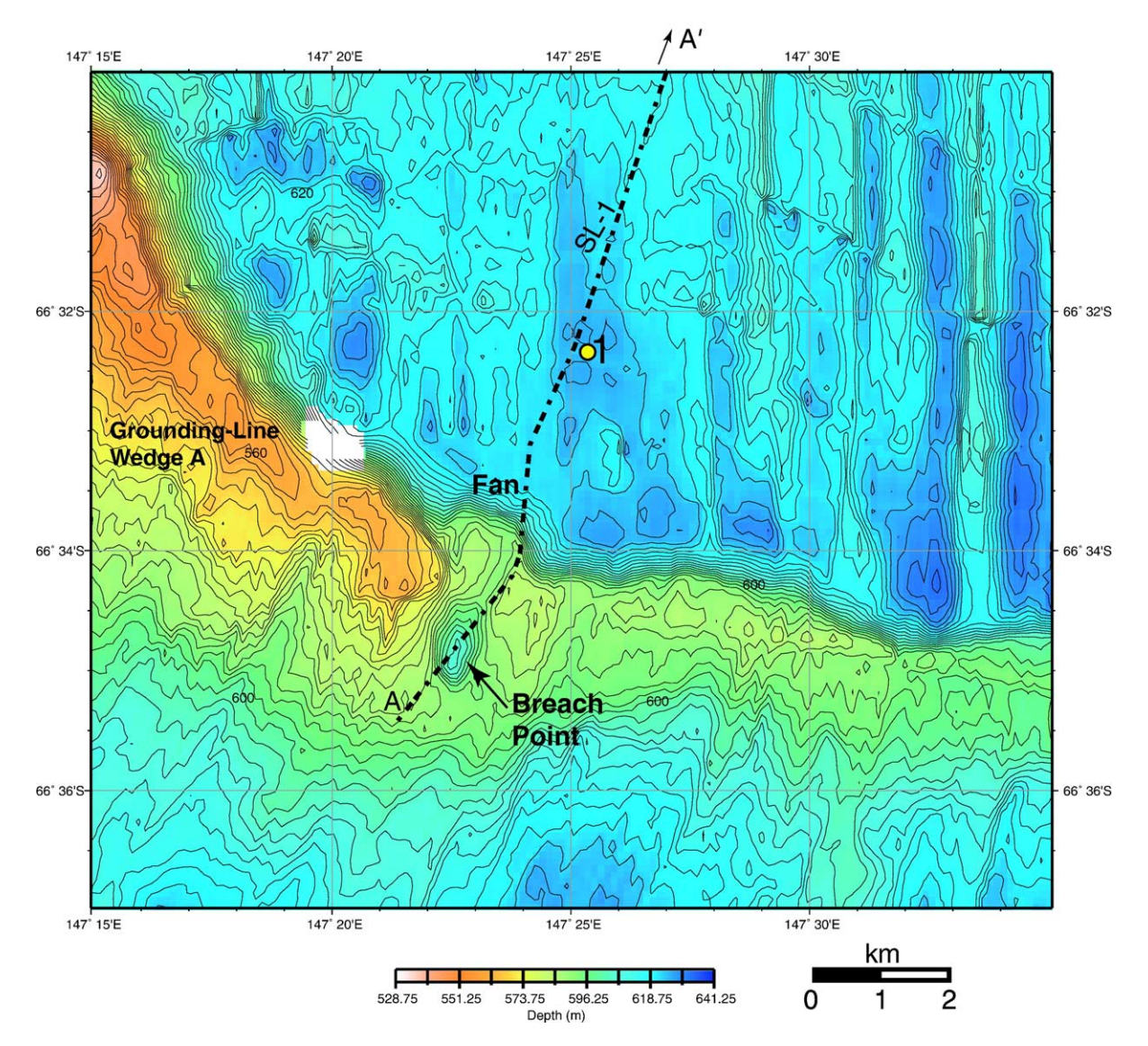


Fig. 3. Detailed bathymetry map of breach point in grounding-line wedge A. A fan of sediment can be seen to the north of the breach point. Bathymetric contours are in 2.5 m intervals.

and have a smooth sinuous contour, while the south-western sides have a gentle slope and show numerous ridges and valleys. These are most likely extensions of the Mertz Moraine(s), located to the west on the Mertz Bank (Eittreim et al., 1995).

Within grounding-line wedge A, there is a depression that is 15 m deep, referred to as a breach point (Figs. 2–4). Associated with this depression is an apparent fan of sediment extending seaward beyond the otherwise smooth contour of the ridge. In line with the breach point, there is a corresponding, but much deeper, indentation in grounding-line wedge B. This depression has a wider diameter and is set back further from the grounding-line wedge crest than the first depression. There is no fan associated with this depression.

Interestingly, the mega-scale glacial lineations in the Mertz Trough are reflected on both the northern and southern sides of the grounding-line wedges; although, they are best developed north of grounding-line wedge A. On the south side of grounding-line wedge A, the ridges are oriented north northeasterly and they are wider and not as long or tall as those to the north, indicating that they are not as prominent.

3.1.3. Sediment structure

In seismic line SL-1, from $66^{\circ}24'$ S, $147^{\circ}35'$ E to $66^{\circ}36'$, $147^{\circ}20'$ E, we have identified three acoustic units (Fig. 4). Unit 1, which extends down from the sediment—water interface to an unconformity, $U_{1,2-3}$, and Unit 2, is up to 6 m thick on this seismic line. Unit 1 contains parallel reflectors that onlap onto $U_{1,2-3}$ and Unit 2. Unit 1 tends to get thinner at the tops of

ridges and eventually pinches out at the northeast end of the line. Unit 2 is located in the seaward direction of grounding-line wedge A, underneath Unit 1 and onlaps onto the underlying unconformity. Unit 2 reaches up to 6 m thick. Below the unconformity, lies Unit 3, which has a hummocky surface that is partially masked by overlying units and lacks strong internal reflectors. Flutes are seen on Unit 3 in the mega-scale glacial lineations area.

The seismic data show that most accumulation of Unit 1 occurs in the trough's deepest areas (Fig. 4). In the region of mega-scale glacial lineations, the sediment is thickest in the scours, where it may reach 7 or more meters. The ridges have the thinnest layers of sediment, ranging from about 2–5 m. Contour lines of the sediment cover thickness closely follow depth contour lines, showing the influence of bathymetry on the sediment cover.

The sediment cover in the grounding-line wedge zone is also affected by trough bathymetry, much like the mega-scale glacial lineation region. There is little sediment on the ridge crests and thickness increases with depth. KC-2, taken on top of grounding-line wedge B, shows only about half a meter of Unit 1 sediment above Unit 3; however, other areas on the grounding-line wedge crests have up to 2 m of sediment overlying Unit 3. Scours in between the ridges have thicker sediment cover of about 12–15 m.

3.1.4. Sediment properties

KC-1, KC-12, and KC-13 are composed of Unit 1, a diatom mud and ooze, which is further divided into two

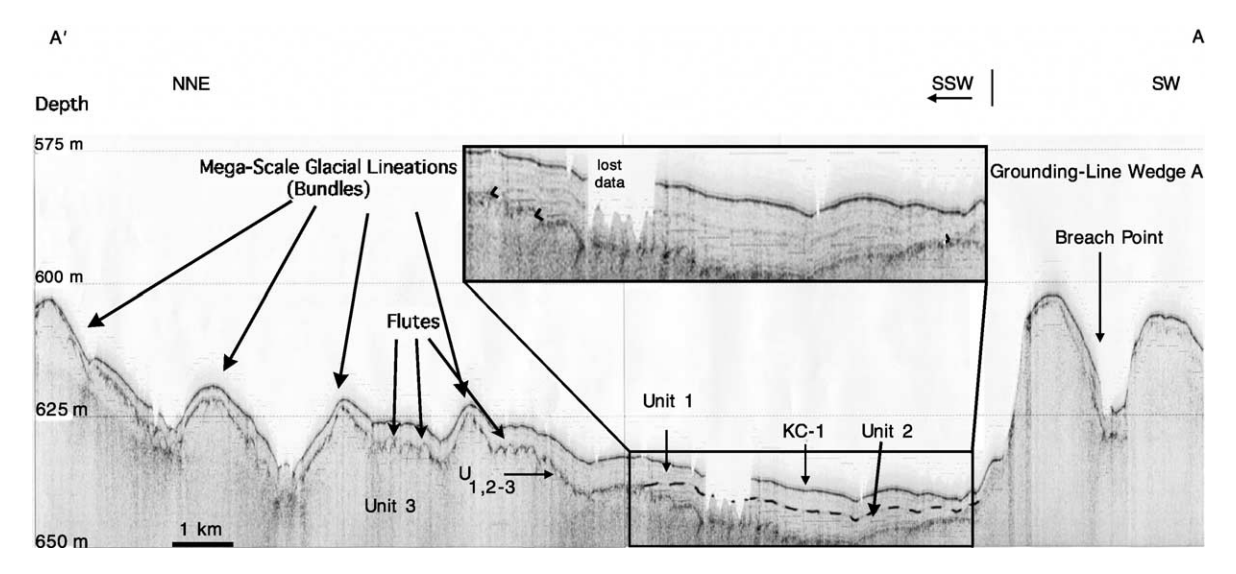


Fig. 4. Seismic line of mega-scale glacial lineations, sediment fan, and breach point in grounding-line wedge A. Units 1, 2 and 3 are shown. Magnification of fan area (Unit 2) has arrows showing onlapping reflectors of Unit 2 onto Unit 3. Location of line shown in Fig. 2.

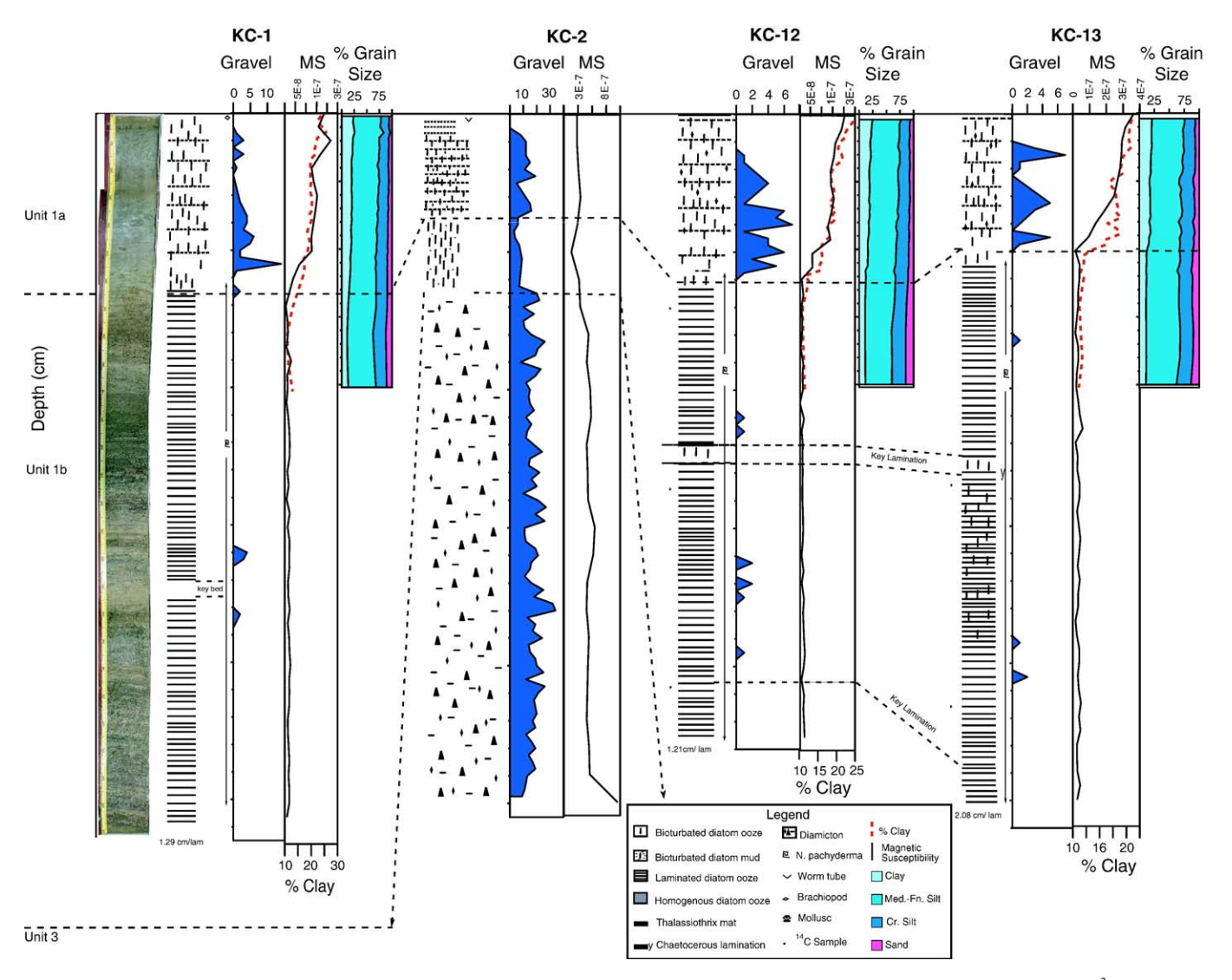


Fig. 5. Fence diagrams with data obtained from the kasten cores in the Mertz Trough. Gravel is measured in grains/2.5 cm interval and magnetic susceptibility in m³/kg. Grain size percentages are based on the finer fraction of the sediment only and do not include gravel. A fining upwards can be seen in the upper 100 cm of KC-1, KC-12, and KC-13. KC-1 core photograph shows transition between Unit 1a and Unit 1b. Unit 1a is the uppermost unit in all four cores, which overlays Unit 1b, the lowermost unit in KC-1, KC-12, and KC-13. KC-2 shows a condensed section of Unit 1 and reaches into Unit 3.

sub-units (Fig. 5). Unit 1a is a grayish olive, clay-rich diatom mud with ice-rafted debris and high magnetic susceptibility. Unit 1b, a thin to thickly laminated diatom ooze, lacks the siliclastic component found in Unit 1a. Unit 1b ranges in color including: grayish olive, light olive brown, moderate olive brown, olive gray, dusky yellow, and yellowish gray. KC-2 reaches into Unit 3, an olive gray, structureless diamicton with occasional soft sediment clasts or clots. These units correspond to units reported on by Presti et al. (2003) on the Mertz Drift, further to the west. Our Unit 1a corresponds to their Unit 4, our Unit 1b to their Unit 3, and our Unit 3 to their Unit 1.

Susceptibility is generally low throughout this suite of cores, ($<4\times10^{-7}~\text{m}^3/\text{kg}$), indicating the high abundance of paramagnetic and diamagnetic materials. Mass normalized magnetic susceptibility of the Mertz Trough cores reflects variations in the lithostratigraphy, and can be used to help define the sedimentary units (Fig. 5). Within homogeneous Unit 1a, magnetic susceptibility varies from $1-4\times10^{-7}~\text{m}^3/\text{kg}$. Within laminated Unit 1b, mass normalized magnetic susceptibility drops by one order of magnitude.

The grain size of cores KC-1, KC-12, and KC-13 show a fining upwards sequence within the top 100 cm (Fig. 5). The percentages of clay in these cores increase from about 15% to 25% towards the top as the percentages of coarse silt decrease by as much as one third. Although the percentage of medium to fine silt varies in small intervals, it stays relatively the same throughout the cores.

The gravel counts from the top 50 centimeters of KC-12 and KC-13 show three prominent peaks (Fig. 5). These peaks occur in the diatom mud at the top of the cores. As well, these cores have smaller non-correlative peaks within the diatom ooze at various depths.

The peaks of gravel in KC-2 are not as prominent as the most prominent ones within the other cores. KC-2 shows a condensed stratigraphy in the diatom mud that overlies a unit of diamicton. Thus, the gravel count for the lower part of the core is much higher than those of KC-1, KC-12 and KC-13.

Absolute and relative diatom abundance for representative species in KC-12 and KC-13 are presented in Fig. 6. A clear difference in diatom abundance and species assemblage is observed between Unit 1a versus Unit 1b. Unit 1b has high average absolute diatom abundance and is dominated by species of *Chaetoceros*, including both subgenera, the small *Hyalochaete* and larger *Phaeoceros*. Unit 1a, in contrast to Unit 1b, has lower absolute diatom abundance and is dominated by species such as *Fragilariopsis curta*, *Fragilariopsis sublinearis*, and *Porosira glacialis*.

3.1.5. Dating

Samples of sediment from each kasten core and several mollusc calcite samples from KC-1 were used to determine ¹⁴C ages, which were calculated using the methods of Stuiver and Polach (1977, Table 2). The sedimentation rate was calculated using the ¹⁴C ages. The sedimentation rate in Unit 1a was calculated using dates from organic matter. Though there is a surface

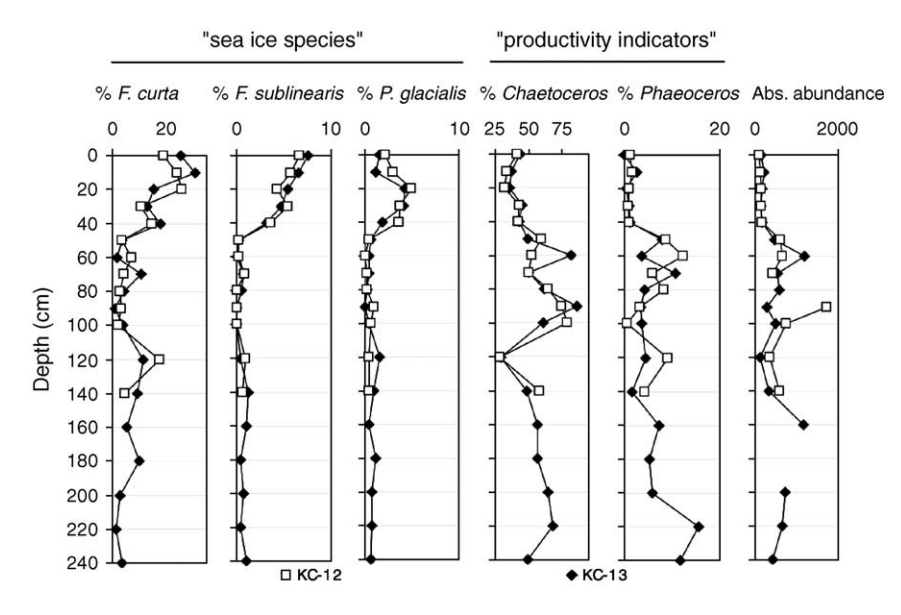


Fig. 6. Relative abundance data for several species of diatoms from KC-12 (open squares) and KC-13 (filled diamonds). Absolute abundance data are measured in millions of valves per gram dry sediment.

Table 2 Uncalibrated ¹⁴C dates of core samples

Core	Depth (cm)	Lab #	¹⁴ C age	Lab	Carbon source
			(yr BP)	error ±	
KC-1	0-2	79839	3410	40	aiom
KC-1	1	85741	920	35	Mollusc calcite
KC-1	30-31	85802	4950	50	aiom
KC-1	68-69	79840	5650	40	aiom
KC-1	106	85742	5380	80	Mollusc calcite
KC-1	122-140	85743	5470	35	Mollusc calcite
KC-1	160-161	85803	5935	50	aiom
KC-1	200	85744	5755	35	Mollusc calcite
KC-1	247	85745	4750	110	Mollusc calcite
KC-1	247-248	79841	6220	40	aiom
KC-2	0-2	79842	4360	50	aiom
KC-2	50-52	79843	6240	50	aiom
KC-12	68-70	79844	5590	40	aiom
KC-12	138-140	85804	6005	40	aiom
KC-12	220-222	79845	6110	40	aiom
KC-13	60-62	79846	5360	50	aiom
KC-13	140-142	85805	5975	40	aiom
KC-13	233-235	79847	5980	40	aiom

 $[\]delta^{13}$ C is assumed.

shell sample, there are no other shell samples in Unit 1a that can be used to calculate a sedimentation rate. The sedimentation rate in Unit 1b was calculated using both shell and organic matter dates, both of which produced the same rate. The sedimentation rate in Unit 1b is about 0.2 cm/yr where as in Unit 1a it is about 0.02 cm/yr, an order of magnitude lower (Fig. 7). By extrapolating the sedimentation rate of Unit 1a to its bottom depth in KC-1 (65 cm) we calculate that Unit 1a started to be deposited 3250 ¹⁴C yr BP. This seems to coincide with the onset of the Neoglacial as recorded in the Palmer Deep 3360 calendar years BP (Domack et al.,

2001). Though the extrapolated line of Unit 1a sediment rate shows an older onset date than the dates in the top of Unit 1b, Unit 1a is more influenced by reworking of sediment and these sample ages have not been corrected for reservoir age.

4. Discussion

The seafloor morphology of the Mertz Trough shows abundant evidence of bed shaping by glacial ice. Mega-scale glacial lineations in the Mertz Trough are evidence of past ice streaming. Moving ice is assisted by a deformable till bed (Anderson et al., 2001), which acts as a lubricant and allows ice above it to move rapidly, thus forming an ice stream. An ice stream once drained the Mertz and Ninnis glacier systems, both of which flowed northward through the Trough. A change in flow direction of the ice sheet is reflected in the orientation and prominence of megascale glacial lineations. The ridges on the south side of the grounding-line wedge are not as prominent and have a different orientation than those to the north, but individual lineations in the north correspond to those in the south. This could be due to a change in the substrate, which would affect the velocity of the ice. This might also be due to adaptation to basal morphology or possibly a change in flow direction with time. However due to the continuation of individual lineations on either side of the grounding-line wedge, we interpret that the basal ice processes were unchanged.

Interpreted erosional features occur in the Mertz Trough in the form of a breach point on grounding-line wedge A and an indentation on grounding-line

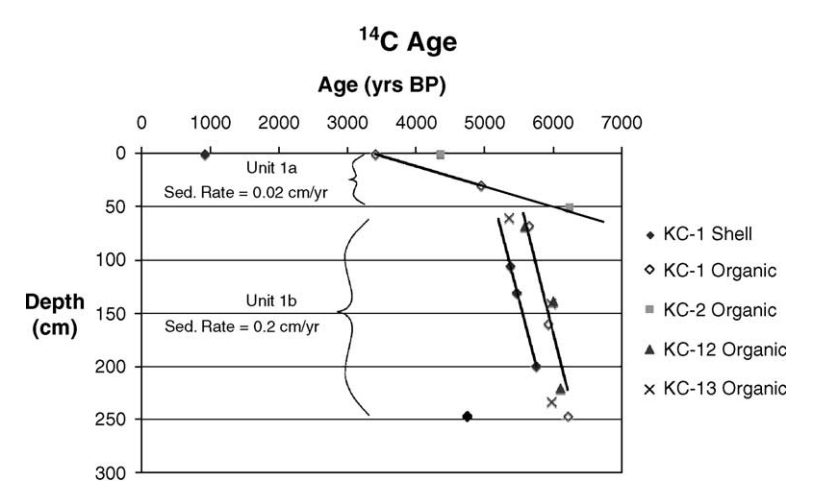


Fig. 7. ¹⁴C ages of sediment samples. The sedimentation rate of Unit 1a is about 0.02 cm/yr and Unit 1b is about 0.2 cm/yr, both were calculated from uncorrected ages.

wedge B. We infer that the breach point formed from subglacial meltwater that breached the grounding-line wedges. The sediment-laden water eroded a hole in the ridge and formed a fan below and seaward of the ridge (Powell and Domack, 2002). The fan of sediment is thickest in its western side (Fig. 3). Assuming that an ice shelf was present seaward of the grounding line, it can be inferred that the Coriolis force effect on sub ice shelf water circulation deflected sedimentladen water to the west producing an asymmetry of the depocenter (Williams et al., 1998; Harris, 2000). Grounding line fans are composed of deposits from subaquatic outwash, sediment gravity flow and suspension settling (Powell and Domack, 2002). The NBP01-01 cruise attempted to take a 20 m jumbo piston core of the distal portions of the fan; however, upon pullout the core failed to retain the sediment it collected due to the cohesive clay making up the sediment in this area.

The breach point in grounding-line wedge A had an effect on subsequent grounding-line positions. The indentation in grounding-line wedge B is much larger than the breach point in grounding-line wedge A. It is located along the same flow path, but in a landward direction. It is a much broader feature and lacks a clear fan channel. This suggests that a meltwater stream with a higher volume of water formed it. However, there is no distinguishable fan of sediment associated with the indentation like there is with the breach point, perhaps because the higher water volume distributed sediment over a much larger area.

Seismic lines and core stratigraphy in the Mertz Trough show thicker sediment cover in deeper regions of the Trough and thinner cover in shallower regions. With the margin of the ice in the Mertz Trough, sediment was preferentially deposited in deeper parts of the basin due to gravity. After the glacier retreated and moved out of the region, sediment continued to accumulate more in deep areas than in shallower ones. Preferential deposition of sediment is not due to slumping or gravity flows, as graded beds are not present. Instead, Unit 1b in cores KC-1, KC-12 and KC-13 was visibly laminated. Bottom currents could be concentrating hemipelagic sediment in the scours and eroding or preventing sediment from accumulating on ridges. These sediment deposits are similar to contourite drifts seen in the Prince Gustav Channel, which are controlled by bottom currents (Camerlenghi et al., 2001), though they form in the deeper areas as opposed to on ridges like the contourites.

Results of the magnetic susceptibility, gravel count, grain size, and diatom counts, as well as the stratigra-

phies of cores and seismic lines show that there are three different units that make up sedimentation in the Mertz Trough. These units are based on changes in parameters that occur within the same depth of any one core. The units and subunits occur in similar depths in cores KC-1, KC-12, and KC-13, where as KC-2 shows a condensed section of Unit 1 relative to the other cores.

4.1. Unit 1a

The percentages of clay in cores KC-1, KC-12, and KC-13 show sharp increases around 50–70 cm from underlying sediment. This is also where magnetic susceptibility increases, reflecting a greater proportion of terrigenous sediment. Ice-rafted debris increases in this section as well, suggesting a period of calving icebergs, with distinct pulses of ice-rafted debris. Icebergs break off from the ice sheet or ice tongue and move seaward where they melt and release any debris, which is deposited in the mud. Thus, there was a change in the nature and source of the sediment that was deposited at the onset of Unit 1a. A re-advance of the Mertz and Ninnis Glaciers could be the reason for greater terrigenous sediment. Additional ice could lead to decreased biological productivity.

A sea ice diatom assemblage dominates Unit 1a. *F. curta*, in particular, has been used as an indicator of sea ice due to its abundance in both sea ice and ice edge blooms (Leventer, 1998). Reports of *F. sublinearis*, summarized by Armand (1997) show that it is typically found in land-fast ice, and less commonly from packice settings. Previously, it has been grouped with sea ice taxa in palaeoenvironmental reconstructions (Barcena et al., 1998). The environmental preferences of *P. glacialis* are less well known, probably because of its generally low relative abundance in sediments of the Southern Ocean (Armand, 1997). However, Armand (1997) notes that *Porosira* abundances increase with extensive annual sea ice cover.

4.2. Unit 1b

Unit 1b, a diatom ooze, is coarser grained than Unit 1a and has lower magnetic susceptibility. It is composed mostly of material that comes from a biologic origin. The *Hyalochaete* diatoms in Unit 1b, which include both vegetative cells and resting spores, traditionally have been interpreted as representing regions of very high primary productivity, usually in the spring (Leventer et al., 1996 and references therein). This interpretation is based on

both field observation (Karl et al., 1991; Leventer, 1991) and laboratory experiments (e.g., French and Hargraves, 1980). Controls on the distribution of the subgenus Phaeoceros, are less well understood. We note that in Unit 1b, large and fragile diatom taxa, including Phaecoeros (Fig. 6), Trichotoxon reinboldii, and Thalassiothrix are common. Their occurrence is notable since in general, these species are rarely preserved in sediments. As discussed in Leventer et al. (2002), the abundance of these large diatoms (as observed in laminations from the Palmer Deep, Antarctic Peninsula) may be a function of long periods of upper water column stratification during the summer, followed by rapid settling once stratification breaks down in the fall. In Unit 1b, higher biogenic productivity as indicated by the diatom data is also reflected in the lower magnetic susceptibility signal and increased sedimentation rates.

4.3. Deposition of terrigenous material

The fining upwards sequence in the top 100 cm of cores KC-1, KC-12, and KC-13 reflects a decrease in diatom-sourced sediment and an increased predominance of terrigenous material. The clay percentage closely follows the magnetic susceptibility, suggesting clay is the iron-carrying fraction of the sediment. The amount of terrestrial input is from fine fractions of the sediment and coarse ice-rafted debris. Terrestrial input has increased roughly within the past 3000 yr, during the deposition of Unit 1a. The coarse silt and sand components of the sediment mostly consist of diatom frustules. The percentages of these grain sizes decrease upwards, which along with the diatom data indicates the diatom productivity is decreasing with time. As well, the sediment accumulation rate drops at the onset of Unit 1a deposition, indicating an increase in terrigenous material is not likely masking the biogenic sediment, even though terrigenous material is more prevalent.

The Ninnis Glacier Tongue could be a possible source for the clay portion of the sediment in Unit 1a. The percentage of clay in KC-1 is slightly higher than that of KC-12, which is still higher than the percentage of clay in KC-13 (Fig. 5). KC-1 is on the seaward side of the Mertz Trough, where as KC-13 is on the landward side of the trough. Sediment at the base of ice shelves can freeze on to the shelf near the grounding line and be released via undermelt near the calving line. If the Ninnis Glacier Tongue had basal freezing near the grounding line, then most of the sediment deposited by the ice shelf would come from

the outermost portion, near the calving line. Thus, water currents could be transporting sediment from the Ninnis Glacier Tongue to the Mertz Trough. The coarser particles tend to fall out of suspension before finer particles because of their higher density. Thus, coarse sediments will be deposited close to the calving line and finer sediments will not fall out of suspension until they are further offshore. The majority of the fine sediment that is deposited in the Mertz Trough should occur in the seaward side of the trough, whereas smaller amounts of fine-grained sediment should be deposited in the landward side of the trough. This is supported by the relationship of the clay percentages in the cores from the Mertz Trough.

This process of deposition is different from that proposed in the Mertz Drift, by Presti et al. (2003), where sediment is thought to be deposited by upwelling Modified Circumpolar Deep Water that winnows sediments on the outer shelf and deposits them as the current slows. The coarser sediments are deposited near the outer shelf and finer sediments fall out of suspension closer to the inner shelf (Presti et al., 2003). At least in the Mertz Trough, the grain-size data from sediment cores show no evidence of this process, as finer sediment is located in cores closer to the outer shelf.

5. Conclusion

An ice sheet once covered the Mertz Trough producing depositional and erosional features. During glacial maximum, an ice stream flowed directly north, as shown by mega-scale glacial lineations. At this time diamicton (Unit 3) was being deposited. During ice retreat, grounding-line wedge A was deposited. Subglacial meltwater eroded a breach point into the grounding-line wedge and deposited a fan of sediment (Unit 2) seaward of the breach. The glacier continued to retreat and mega-scale glacial lineations landward of grounding-line wedge A suggest that the ice stream was not as prominent during this time. The glacier paused and deposited grounding-line wedge B. After the ice retreated, a diatomaceous mud and ooze (Unit 1) was deposited. First as laminated diatom ooze (Unit 1b). Then, about 3300 yr BP, a diatomaceous mud containing more ice-rafted debris, higher clay percentages, and higher magnetic susceptibility values was deposited (Unit 1a). Three distinct episodes of iceberg calving took place, depositing coarse-grained ice-rafted debris. Unit 1 was preferentially deposited in deeper parts of the trough. Diatom mud lacking ice-rafted debris has been deposited most recently.

Acknowledgements

This research was made possible from the financial support of the National Science Foundation Office of Polar Programs grant No. 9909367 to Amy Leventer, 9909837 to Rob Dunbar, and 9909803 to Stefanie Brachfeld. Pat Reynolds assisted by providing insight to potential biological processes occurring in the Mertz Trough. Kathleen Gavahan produced swath maps of the Mertz Trough. This manuscript has benefited greatly from reviews by Angelo Camerlenghi and an anonymous reviewer.

References

- Anderson, J.B., Wellner, J.S., Lowe, A.L., Mosola, A.B., Shipp, S.S., 2001. Footprint of the expanded West Antarctic ice sheet: ice stream history and behavior. GSA Today 11 (10), 4–9.
- Armand, L.K., 1997. The use of diatom transfer functions in estimating sea-surface temperatures and sea-ice in cores from the southeast Indian Ocean. Ph.D. Dissertation, Australian National University. 392 pp.
- Barcena, M.A., Gersonde, R., Ledesma, S., Fabres, J., Calafat, A.M., Canals, M., Sierro, F.J., Flores, J.A., 1998. Record of Holocene glacial oscillations in Bransfield Basin as revealed by siliceous microfossil assemblages. Antarctic Science 10 (3), 269–285.
- Barnes, P.W., 1987. Morphologic studies of the Wilkes Land Continental Shelf, Antarctica—glacial and iceberg effects. In: Eittreim, S.L., Hampton, M.A. (Eds.), The Antarctic Continental Margin: Geology and Geophysics of Offshore Wilkes Land, CPCEMR Earth Science Series, 5A. Circum-Pacific Council for Energy and Mineral Resources, Houston, Texas, pp. 175–194.
- Benn, D.I., Evans, D.J.A., 1998. Glaciers and Glaciation. Arnold, London. 734 pp.
- Camerlenghi, A., Domack, E., Rebesco, M., Gilbert, R., Ishman, S., Leventer, A., Brachfeld, S., Drake, A., 2001. Glacial morphology and post-glacial contourites in northern Prince Gustav Channel (NW Weddell Sea, Antarctica). Marine Geophysical Researches 22, 417–443.
- Canals, M., Urgeles, R., Calafat, A.M., 2000. Deep sea-floor evidence of past ice streams off the Antarctic Peninsula. Geology 28 (1), 31–34.
- Domack, E.W., 1987. Preliminary stratigraphy for a portion of the Wilkes Land Continental Shelf, Antarctica: evidence from Till Provenance. In: Eittreim, S.L., Hampton, M.A. (Eds.), The Antarctic Continental Margin: Geology and Geophysics of Offshore Wilkes Land, CPCEMR Earth Science Series, 5A. Circum-Pacific Council for Energy and Mineral Resources, Houston, Texas, pp. 195–203.
- Domack, E.W., Jacobson, E.A., Shipp, S.S., Anderson, J.B., 1999.
 Late Pleistocene/Holocene retreat of the West Antarctic ice sheet in the Ross sea: Part 2. Sedimentologic and stratigraphic signature. Geological Society of America Bulletin 111, 1517–1536.
- Domack, E., Leventer, A., Dunbar, R., Taylor, F., Brachfeld, S., Sjunneskog, C., 2001. ODP Leg 178 scientific party. Chronology

- of the Palmer Deep site, Antarctic Peninsula: a Holocene palaeoenvironmental reference for the circum-Antarctic. Holocene 11 (1), 1-9.
- Eittreim, S.L., Cooper, A.K., Wannesson, J., 1995. Seismic stratigraphic evidence of ice-sheet advances on the Wilkes Land margin of Antarctica. Sedimentary Geology 96 (1–2), 131–156.
- French, F.W., Hargraves, P.E., 1980. Physiological characteristics of plankton diatom resting spores. Marine Biology Letters 1, 185–195.
- Grobe, H., 1987. A simple method for the determination of ice-rafted debris in sediment cores. Polarforschung 3 (57), 123–126.
- Harris, P.T., 2000. Sedimentological signatures of sub-ice-shelf circulation: an example from Vincennes Bay, East Antarctica. Papers and Proceedings of the Royal Society of Tasmania, vol. 133 (3), pp. 57–62.
- Karl, D.M., Tilbrook, B.D., Tien, G., 1991. Seasonal coupling of organic matter production and particle flux in the western Bransfield Strait, Antarctica. Deep-Sea Research 38, 1097–1126.
- Leventer, A., 1991. Sediment trap diatom assemblages from the northern Antarctic Peninsula region. Deep-Sea Research 38, 1127–1143.
- Leventer, A., 1998. The fate of Antarctic "sea ice diatoms" and their use as paleoenvironmental indicators. In: Lizotte, M.P., Arrigo, K.R.Antarctic Sea Ice: Biological Processes, Interactions and Variability, Antarctic Research Series, vol. 73, pp. 121–137.
- Leventer, A., Domack, E.W., Ishman, S.E., Brachfeld, S., McClennen, C.E., Manley, P., 1996. Productivity cycles of 200–300 years in the Antarctic Peninsula region: understanding linkages among the sun, atmosphere, ocean, sea ice and biota. GSA Bulletin 108 (12), 1626–1644.
- Leventer, A., Domack, E.W., Barkoukis, A., McAndrews, B., Murray, J., 2002. Laminations from the Palmer Deep; a diatom-based interpretation. Paleoceanography 17 (3).
- Porter-Smith, R., 2003. Bathymetry of the George Vth land shelf and slope. Deep-Sea Research II 50, 1337–1341.
- Powell, R., Domack, E., 2002. Modern glaciomarine environments. In: Menzies, J. (Ed.), Modern and Past Glacial Environments. Butterworth-Heinemann, Boston, pp. 361–389.
- Presti, M., De Santis, L., Busetti, M., Harris, P.T., 2003. Late Pleistocene and Holocene sedimentation on the George V continental shelf, East Antarctica. Deep-Sea Research II 50, 1441–1461.
- Scherer, R.P., 1995. A new method for the determination of absolute abundance of diatoms and other silt-sized sedimentary particles. Journal of Paleolimnology 12, 171–178.
- Shipp, S., Anderson, J., Domack, E., 1999. Late Pleistocene–Holocene retreat of the West Antarctic ice-sheet system in the Ross Sea: Part 1. Geophysical results. GSA Bulletin 111 (10), 1486–1516.
- Stuiver, M., Polach, H.A., 1997. Discussion: reporting of C-14 data. Radiocarbon 19, 355–363.
- Wellner, J.S., Lowe, A.L., Shipp, S.S., Anderson, J.B., 2001. Distribution of glacial geomorphic features on the Antarctic continental shelf and correlation with substrate: implications for ice behavior. Journal of Glaciology 47 (158), 397–411.
- Williams, M.J.M., Warner, R.C., Budd, W.F., 1998. The effects of oceanwarming on melting and ocean circulation under the Amery Ice Shelf, East Antarctica. Annals of Glaciology 27, 75–80.